Title

High Spatiotemporal Resolution Imaging with Localized Plasmonic Structured Illumination Microscopy

Journal

ACS Nano, 12(8)

ISSN

1936-0851

Authors

Bezryadina, Anna
Zhao, Junxiang
Xia, Yang
et al.

Publication Date

2018-08-28

DOI

10.1021/acsnano.8b03477

Peer reviewed

ACS NANO
Cite This: ACS Nano XXXX, XXX, XXX−XXX
www.acsnano.org

ARTICLE

High Spatiotemporal Resolution Imaging with Localized Plasmonic Structured Illumination Microscopy

Anna Bezryadina,[†] Junxiang Zhao,[†] Yang Xia,[‡] Xiang Zhang,[‡] and Zhaowei Liu*[,†]

[†]Department of Electrical and Computer Engineering, University of California, San Diego, La Jolla, California 92093, United States
[‡]Department of Mechanical Engineering, University of California, Berkeley, Berkeley, California 94720, United States

Supporting Information

ABSTRACT: **Localized plasmonic structured illumination microscopy (LPSIM) provides multicolor wide-field super-resolution imaging with low phototoxicity and high-speed capability. LPSIM utilizes a nanoscale plasmonic antenna array to provide a series of tunable illumination patterns beyond the traditional diffraction limit, allowing for enhanced resolving powers down to a few tens of nanometers. Here, we demonstrate wide-field LPSIM with 50 nm spatial resolution at video rate speed by imaging microtubule dynamics with low illumination power intensity. The design of the LPSIM system makes it suitable for imaging surface effects of cells and tissues with regular sample preparation protocols. LPSIM can be extended to much higher resolution, representing an excellent technology for live-cell imaging of protein dynamics and interactions.**

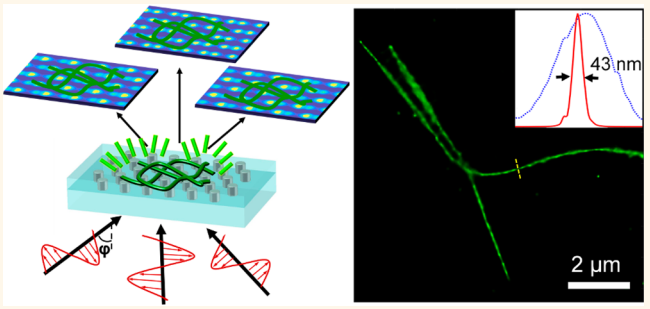

KEYWORDS: *super-resolution microscopy, plasmonics, structure illumination microscopy, live-cell imaging, nanofabrication, LPSIM*

Live observation of cell signaling pathways, immune responses, surface events during cell cycle and adhesion, and movement of proteins and calcium ions inside live cells is essential to understand cell dynamics, biochemical activities, and response to internal and external stimuli. Fixed biosamples can be observed at nanometer accuracy with X-ray and scanning electron microscopy (SEM) imaging, but live-cell resolution is limited to around 200 nm due to the diffraction limit of optical microscope systems. To visualize and detect the motion and interaction of nanoscale features and to image cytoskeletal structures in living cells, different proteins can be fluorescently marked with different colors by using self-labeling proteins tags,[1,2] genetically encoded markers such as fluorescent proteins,[3] synthetic organic fluorophores,[3] or engineered probes coupled to ligands that bind to specific proteins.[4] To observe sub-diffraction-limited biostructures, a number of super-resolution microscopy techniques[1,5] have been developed during the past decade, including structured illumination microscopy (SIM),[6,7] stimulated emission depletion (STED) microscopy,[8,9] stochastic optical reconstruction microscopy (STORM),[10,11] and photoactivated localization microcopy (PALM).[12] These methods have evolved into new microscopy sub-branches and extended the capability of optical imaging to a new era. However, each of these techniques has trade-offs between resolution, imaging speed, optical power density, and system complexity that limits its practical applications.[1] For instance, localization-based super-resolution techniques are typically very slow. STED usually has a small field of view due to its scanning mechanism, and the high intensity STED beam can potentially damage sensitive biological samples. Standard SIM has a wide field of view, high imaging speed, and relatively low photodamage but with a comparatively low 2 times resolution enhancement compared to the diffraction limit.[6,7,13−21]

SIM illuminates a sample with a sequence of sinusoidal interference patterns of high spatial frequency, which make the fine structures of the sample become visible as moiré fringes. Recent advances in SIM have extended its resolution to 84 nm by combining total internal reflection fluorescence (TIRF) microscopy with a high NA objective to study dynamics in cellular structures.[15] By collecting time-series images of live samples, SIM has demonstrated up to 11 Hz video speed for 2D imaging[7,15] and up to 100 Hz with reduced resolution.[17] Saturated structured illumination microscopy (SSIM) or nonlinear SIM can harvest high-order Fourier components from the nonlinear fluorescent response, leading to much

Received: May 8, 2018
Accepted: July 25, 2018
Published: July 25, 2018

DOI: 10.1021/acsnano.8b03477
ACS Nano XXXX, XXX, XXX−XXX

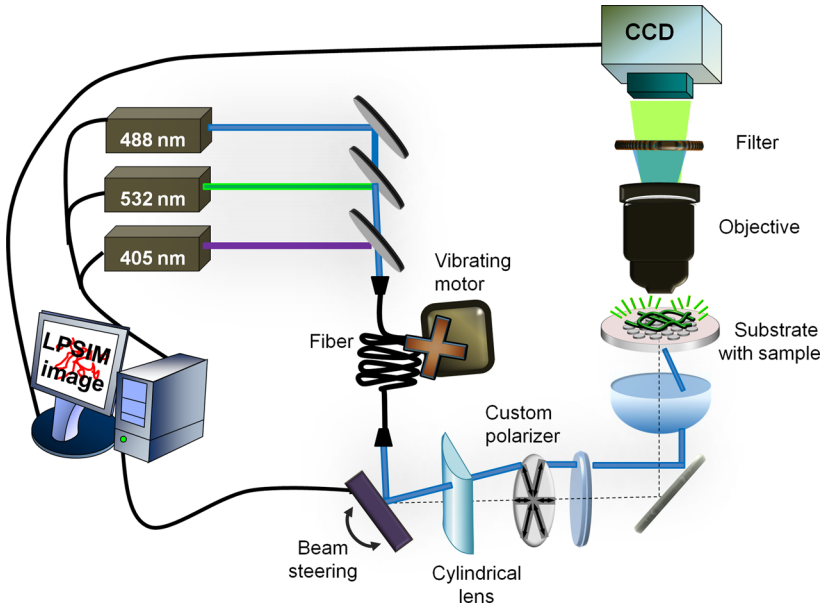

Figure 1. Simplified optical layout of LPSIM microscopy. Beams from three lasers (405, 488, 532 nm) are co-aligned and sent through a multimode fiber. Lasers are controlled with internal shutters and switched simultaneously or sequentially depending on the application. The fiber is vibrated by using two 5 V motors to scramble the modes and remove speckles in the laser beam. After the fiber, the beam (blue line) is collimated and reduced to a ~1.5 mm diameter and sent through a pair of galvo mirrors to steer the beam angle of the illumination. The 4f system of two lenses between galvo mirrors and the sample plane allows precise control of illumination angles, and a cylindrical lens corrects the mismatch in the paths of the 4f system in two axial directions from a pair of galvo mirrors. The custom polarizer ensures TM polarization for all of the illumination angles on the LPSIM substrate. The periodic substrate pattern and microtubules are magnified for illustration purposes. The fluorescent signal from the sample is collected from above with a high NA objective and sent to the sCMOS camera after an excitation laser filter. For multicolor imaging, the excitation laser filter is replaced with a filter wheel.

greater resolution.[18,19] This method, however, inevitably causes strong photobleaching and much slower imaging speed. By combining SSIM with reversible photoswitchable fluorescent proteins, the phototoxicity is reduced, which allows biologically compatible imaging with 50 nm resolution at up to a few Hz frame rate.[19]

Plasmonics provides an opportunity to create periodical illumination patterns beyond the traditional diffraction limit, allowing for SIM with greatly enhanced resolution to study near-surface effects. Plasmonic SIM (PSIM) uses surface plasmon polariton (SPP) interferences at a metallic−dielectric interface to achieve finer illumination patterns and higher resolution.[22−27] Localized plasmonic structured illumination microscopy (LPSIM) utilizes an array of localized plasmonic (LP) antennas to generate the illumination pattern.[28−30] As the LP field is strongly associated with the antenna structure, the LP field can be tuned to contain almost arbitrarily high spatial frequency components in the illumination pattern by adjusting the antenna geometry.[28] LPSIM allows the generation of finer periodically structured illumination patterns, which shifts the high spatial frequency information of the object into the detectable bandwidth of the optical system. The prototype LPSIM system has resolved details down to ~80 nm for fixed neuron cells.[29] Recently, LPSIM has been combined with optically trapped microlenses to further improve its resolution.[30] Properly fabricated plasmonic structures with controlled near-field excitation have the potential to bring the resolution of live-cell imaging down to a few tens of nanometers while preserving the wide field of view, high speed, and low phototoxicity of the SIM system. LPSIM offers a powerful approach to detect live interaction of viruses, vesicles movement in cells, individual antibodies, and intracellular protein signaling with much greater detail.

In this study, we experimentally demonstrate LPSIM imaging for fluorescently tagged specimens with high speed and resolution below 50 nm and identify a pathway to improve spatiotemporal resolution even further for monitoring dynamic processes. To achieve this, we designed a new sapphire LPSIM substrate, added multiple laser excitation capability, changed to a high-speed camera, and developed system synchronization for video speed imaging. We show a 4 Hz LPSIM video of microtubules over a 28 × 28 μm field of view under a laser illumination power density of 10−15 W/cm^2. By increasing the exposure intensity to 100−150 W/cm^2, the LPSIM imaging speed can be increased up to 30−40 Hz. By sequentially switching between different excitation lasers, we also demonstrate multicolor imaging. This method can monitor dynamics of proteins in the cell membranes of neurons, muscles, and other tissues. LPSIM uses a specialized substrate comprising an array of designed plasmonic antennas, but it does not require special sample preparation and handling. Similar to traditional SIM and TIRF, the procedure to use LPSIM is compatible with bioimaging protocols. Cells can be grown directly on LPSIM substrates or transferred just before imaging.

RESULTS

High-Speed LPSIM Imaging of Microtubule Dynamics. As a first demonstration of high-speed LPSIM imaging, we imaged microtubules stained with green fluorophores (488/550 nm) on a silica-based LPSIM substrate[29] at an illumination power density under 10 W/cm^2 (see Figure 1 for experimental setup). We can see clear improvements in resolution after

DOI: 10.1021/acsnano.8b03477
ACS Nano XXXX, XXX, XXX−XXX

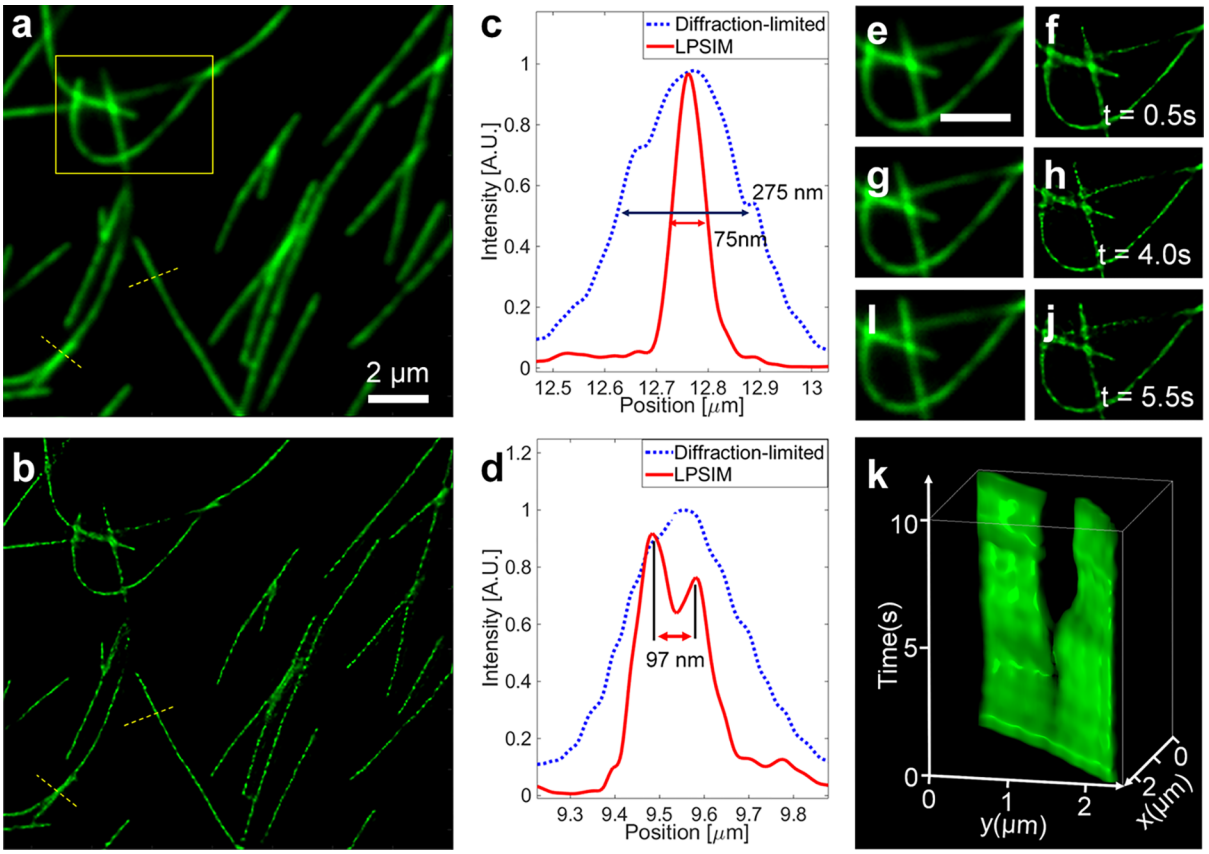

Figure 2. Super-resolution video recording of green microtubule dynamics with LPSIM. (a,b) One frame of wide-field diffraction-limited and LPSIM images, respectively, from a 4 Hz video showing resolution enhancement over the whole field of view (Supporting Movie S1). (c,d) Normalized intensity profiles of the images in (a,b), along the dashed yellow lines. The FWHM of the microtubule is reduced from 275 to 75 nm. (e−j) Snapshots with a closer look at microtubules' movement inside a yellow box in (a) before and after LPSIM. (k) 3D maximum-intensity kymograph of a microtubule breaking apart process from the first 40 LPSIM image frames (Supporting Movie S2).

applying LPSIM, and small movements in the microtubules can be observed (Figure 2a,b and Supporting Movie S1). Figure 2e−j shows a few snapshots of the observed movements before and after LPSIM reconstruction. The full width at half-maximum (FWHM) resolution for this particular video of isolated microtubules is 75 nm in LPSIM, which is slightly more than 3 times better than the diffraction-limited fwhm of the water immersion objective with a numerical aperture (NA) of 1.2 (Figure 2c). Figure 2a,b,d shows two closely spaced microtubules with a 97 nm center-to-center spacing, which can be clearly resolved with LPSIM. By recording a time series of LPSIM frames and visualizing with kymographs, we can evaluate live LPSIM as a tool for distinguishing the growth, shrinkage, movement, and disintegration of microtubules. Figure 2k visualizes the process when one microtubule breaks apart during 40 frames of LPSIM video at a 4 Hz imaging speed (Supporting Movie S2). With kymographs, we can detect and evaluate the precise time and duration of transitions between states.

Less Than 50 nm Resolution with an Ultrahigh NA Objective and New Sapphire LPSIM Substrates. To push the resolution down to 50 nm while retaining high speed and low phototoxicity, we developed a new LPSIM structure on a sapphire substrate, which is designed to be used with an ultrahigh numerical aperture objective (see Methods and Figure S1). By using standard clean room processes including e-beam lithography and thin film deposition, we fabricated several 1 mm^2 uniform hexagonal lattices of 60 nm diameter silver discs with 125, 135, and 145 nm pitches embedded in poly(methyl methacrylate) (PMMA) on top of sapphire cover slides (Figure 3a−c). The optimal size and pitch of the nanodiscs were estimated by simulating their near-field excitation patterns at different incidental illumination angles within the illumination bandwidth of the high NA objective (Figure 3d). The thin PMMA layer protects the silver discs from oxidation and prevents direct contact between the silver and the biological samples. These LPSIM substrates can be reused by washing off the PMMA protection layer with acetone, which also strips away the fluorescent sample, and then recoating the substrate with a new PMMA protection layer.

To characterize the resolving power, green microtubules (488/550 nm) were drop-casted onto the sapphire LPSIM substrate and sandwiched with a coverslip from the bottom. The observation was made in transmission mode with a 100× 1.65 NA high-index oil immersion objectives under 20 W/cm^2 illumination power density (Figure 3). A short 1 Hz video with a 10 × 10 μm field of view is recorded with a 100 ms exposure time (Supporting Movie S3). The LPSIM image produces an astonishing resolution improvement and confinement over conventional fluorescent microscopy, as can be seen both in real space (Figure 3e,f) and Fourier space (Figure 3g,h). In Figure 3i,j, we confirmed the FWHM resolution below 50 nm by the cross-sectional profile at several locations on the new LPSIM design, which corresponds to a resolution on the order of ~λ/11.

DOI: 10.1021/acsnano.8b03477
ACS Nano XXXX, XXX, XXX−XXX

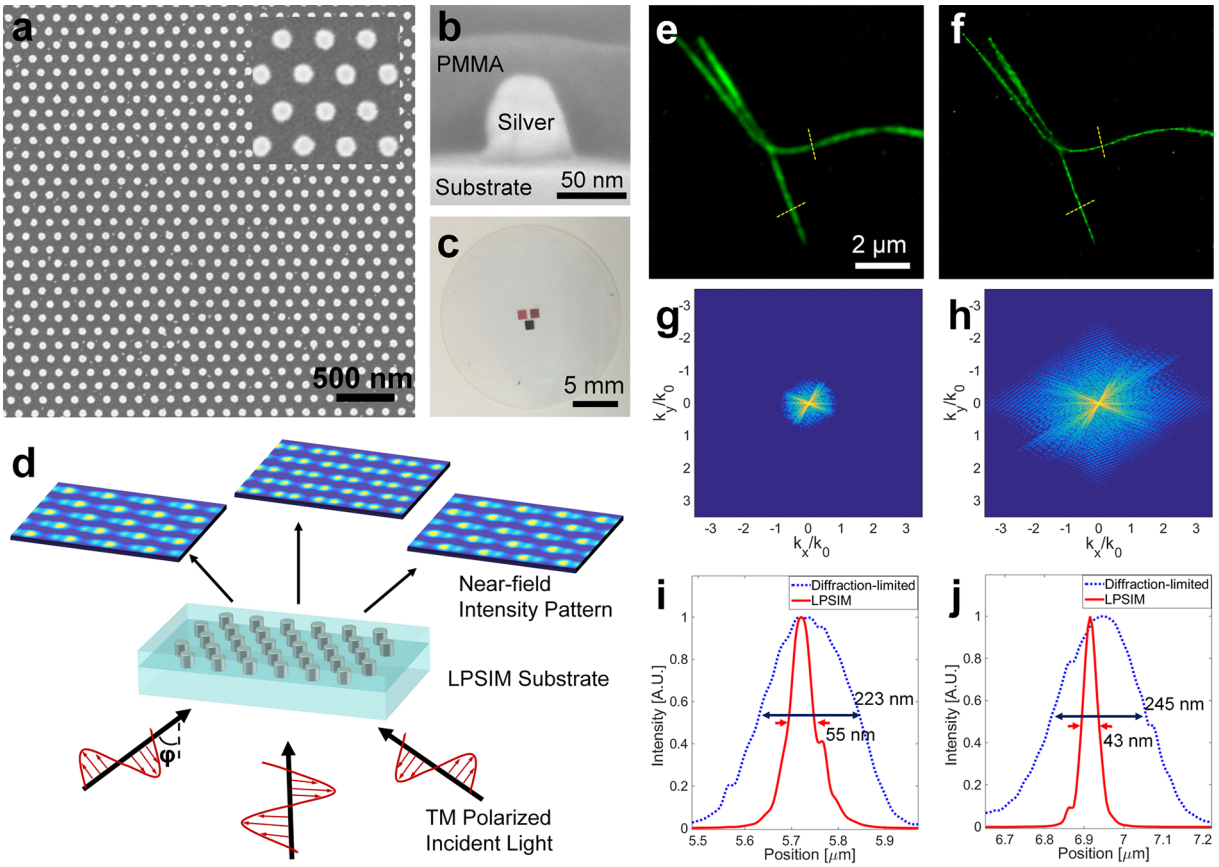

Figure 3. A 50 nm live imaging with LPSIM on a sapphire substrate. (a) Top-view SEM images of the plasmonic antenna array at different magnifications, showing a hexagonal lattice of silver nanodiscs on the sapphire substrate. The disc diameter is 60 nm, and the pitch is 135 nm. (b) SEM cross-sectional image of a 60 nm silver nanodisc on silicon instead of sapphire substrate with PMMA coating to check the fabrication accuracy of the structure. (c) Photograph of the whole sapphire substrate with three patterned antenna array areas with 125, 135, and 145 nm pitch size. (d) Generated near-field intensity patterns on an object plane created by TM-polarized laser beam incident to the 60 nm hexagonal silver disc array on the sapphire substrate at angles of −60, 0, and 60°, along one of the three symmetry axes. (e) Diffraction-limited image of green microtubules. (f) Corresponding LPSIM image of (e) with significantly improved resolution (Supporting Movie S3). (g,h) Spatial frequency spectra (in log scale) of a diffraction-limited and LPSIM image, respectively. The k_0 is the cutoff wave-vector of the diffraction-limited system. The LPSIM technique increases the spatial frequency approximately 3-fold. (i,j) Normalized intensity profile of the images in (e,f) along the dashed yellow lines. The FWHM of the microtubule image is 43 and 54 nm at two different locations.

Multicolor Imaging of Fluorescent Beads. Finally, LPSIM can be readily extended to multiple colors by either illumination with different lasers sequentially or by simultaneous excitation of a multicolor fluorescent sample and recording with split-view devices or an additional camera. Multicolor imaging allows for the study of associated dynamics between multiple fluorescent target species at high spatial and temporal resolution. Here, we demonstrated two color imaging by sequentially switching between 488 and 532 nm lasers and, respectively, exciting 100 nm (505/515 nm) and 45 nm (540/560 nm) diameter fluorescent polystyrene beads, which were drop-casted onto the LPSIM sapphire substrate and imaged with the 1.65 NA 100× objectives (Figure 4). In Figure 4a,c, small clusters of orange and green beads are unresolvable under normal imaging conditions, but under LPSIM, closely spaced multicolored beads are clearly separated (Figure 4b,d). The center-to-center spacing of the orange beads is 70 nm, which implies the edge-to-edge gap between them is 25 nm (Figure 4e), and the FWHM of the green beads is reduced down to 78 nm (Figure 4f). The FWHM of the green bead being less than its physical size of 100 nm is due to the evanescent illumination onto spherically shaped beads (Figure S2).

DISCUSSION

We note several clarifications to the current method. First, the final imaging speed is determined by multiple parameters including the camera readout speed, the illumination pattern modulation speed, and the exposure time (which is also related to light emission efficiency and illumination power density). In the 4 Hz exemplary video, under 10 W/cm^2 illumination, the sCMOS camera requires 5.1 ms to read out each of the nine subimages with 1024 × 1024 pixels; the mirrors require 1.3 ms to change each illumination pattern, and then the camera requires a 20 ms exposure time for each subimage. By reducing the recording area on the camera to 128 × 128 pixels (2.1 × 2.1 μm for 400× magnification) and increasing the illumination power to get enough signal for a 1 ms exposure, the imaging time can be reduced to ∼3.0 ms per subimage, which results in a reconstructed video speed of 37 Hz. With a faster and more sensitive camera and higher sample fluorescence efficiency, the imaging speed for LPSIM can be improved much further beyond 37 Hz.

Second, because the localized plasmonic structure allows for a deep subwavelength confinement of the light, the locally enhanced excitation field extends only about 50−100 nm

DOI: 10.1021/acsnano.8b03477
ACS Nano XXXX, XXX, XXX−XXX

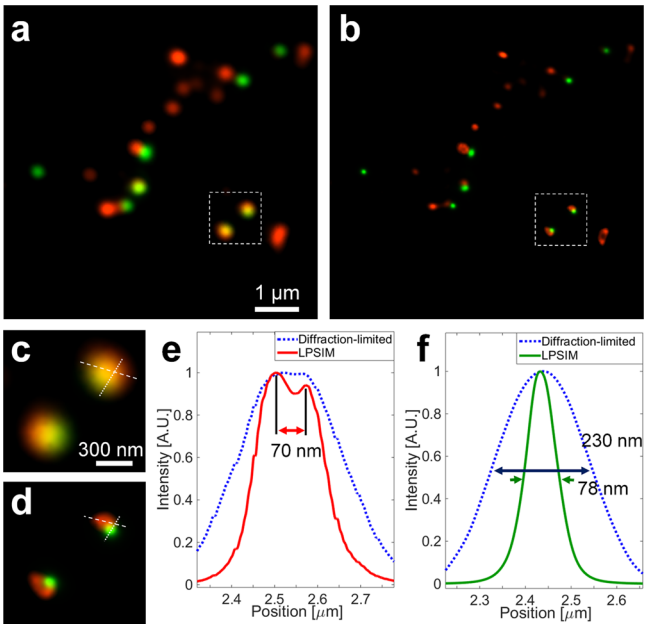

Figure 4. Two color LPSIM demonstration. (a) Diffraction-limited image of a mixture of orange (45 nm in diameter) and green (100 nm in diameter) fluorescent beads. (b) Corresponding LPSIM image of (a) with more than 3 times resolution improvement. (c,d) Closer look at the area inside of the box from (a,b). (e,f) Normalized intensity profile of the pair of orange beads along the dashed white line and a green bead along dot line in (c,d).

inside the specimen, which creates a higher intensity illumination pattern at lower total laser power and limits the phototoxic exposure of biological samples to a small fraction of the tissue volume. The Purcell effect of the plasmonic structure reduces the fluorescence lifetime of the fluorescent molecules, resulting in lower photobleaching in the biological samples.[31−33] When imaging through thick samples, cross-sectioning using postprocessing imaging analysis[34] can be used to remove out-of-plane information. Therefore, long-term observations with high signal-to-noise ratios and short exposure times can be done with LPSIM imaging.

Finally, similar to SIM,[7,15] an important requirement for LPSIM live imaging is that the acquisition time for each subimage of the video sequence should be short enough so that no feature moves more than approximately one reconstructed FWHM length to avoid reconstruction artifacts. That is why it is always better to use high acquisition speed even for long-time observations. To record sparsely sampled long-duration videos, it is critical to minimize motion artifacts during each acquisition. To limit excessive photobleaching, the lasers should be blocked outside of the camera exposure time to provide recovery time for the cells after photoexcitation.

CONCLUSIONS

With the new design of the LPSIM system, we demonstrated a high-speed, large field of view, and long-duration super-resolution video with 50 nm resolution and low photobleaching, which other super-resolution microscopy techniques currently cannot offer. It is worth noting that the 50 nm resolution is not the theoretical limit of the LPSIM method. High-order harmonic peaks of the near-field pattern have the potential to bring even higher spatial frequency information of the object into the detection bandwidth. Combined with reducing the nanoantenna pitch size to 100 nm or less, the LPSIM technique has the potential to push the resolution scale down to 20−30 nm. Ongoing refinements to LPSIM will help to monitor additional high-speed dynamics of microscopic features in their host environment and answer important questions in biology and medicine.

METHODS

High-Speed Multicolored Plasmonic Microscopy. Our microscope system is based on the previously reported transmission mode LPSIM design[29] with modification to achieve high-speed multicolored imaging (Figure 1). To homogenize the illumination beam and remove speckles, the laser light is coupled to a multimode fiber being vibrated at high frequency using offset-weight motors. Then the beam is sent through a Fourier filtering beam cleaner and collimated to a 1−2 mm^2 beam. By using galvo mirrors (Cambridge Technology MicroMax 673) modulated at a maximum 800 Hz speed, we steer the beam and control the incident angle onto the LPSIM substrate. To achieve a controlled high-angle illumination of the plasmonic substrate without a shift of the illumination area, a 4f system of two lenses is used between the galvo mirrors and the focal plane. To guarantee TM polarization for different illumination directions and prevent any time delays with polarization rotation, the beam is sent through a custom-made polarizer plate, which is patterned so that its shape matches precisely with the substrate orientation, before illuminating the sample plane of the Zeiss Axioskop 2 microscope. The fluorescent signal is collected by a high NA objective (60× 1.2 NA water immersion Olympus objective or 100× 1.65 NA oil immersion Olympus objective), sent to the camera with proper laser filters. For optimal prolonged imaging, the substrate with biological samples is illuminated with an intensity of approximately 10 W/cm^2 and recorded by a sCMOS camera (Hamamatsu ORCA_Flash4.0 V3 digital CMOS camera (C13440−20CU)) using an image size of 512 × 512 pixels with two-bit binning and a 20 ms exposure time. The camera capture speed limit is ∼1.72 ms for a 128 × 128 pixel image and ∼6.1 ms for a 1024 × 1024 pixel image (512 × 512 pixel image with two-bit binning to increase sensitivity), which is the main limitation of the final reconstructed speed. For the minimum possible 1 ms exposure time setting, the illumination power needs to be increased to have enough photon counts.

To achieve multicolor imaging, we can either use multiple lasers simultaneously or sequentially switch between colors. For sequential imaging with one camera and multiple emission colors, we can use shutters to switch between laser beams and synchronize with each camera exposure. For multicolor simultaneous imaging, the different emission colors could be split using dichroic mirrors and band-pass filters and then projected into multiple cameras or one camera with a split sensor for different colors.

To synchronize all equipment properly, we use Matlab software to control a DAQ voltage output module (NI-9263) from National Instruments. Illumination angles, polarization, and filters must be switched before triggering the camera to take and save each subimage. By acquiring nine subimages with different illumination angles, one high-resolution LPSIM final image can be recovered with a blind SIM[35] numerical reconstruction method. After all sets of subimages were collected from the camera (or cameras), the software reconstructs high-resolution images (or video) for each color separately, and then multiple color super-resolution images can be overlapped together as needed.

LPSIM Substrates. We use specially designed substrates with a hexagonal pattern of silver nanodiscs and a thin protective layer on top of them. The geometrical parameters of the structures are chosen such that it has three-order rotational symmetry in the *xy*-plane to achieve maximum *k*-space coverage. For visible wavelengths, the designed LPSIM substrate structure consists of a large area of a 2D hexagonal array of 60 nm silver nanoantennas embedded in PMMA or silica substrate, with periodicity (center to center) of 125−150 nm depending on the desired numerical aperture of the system. The different periodicities of the plasmonic structure make the frequency

DOI: 10.1021/acsnano.8b03477
ACS Nano XXXX, XXX, XXX−XXX

shift of the object information match the detection bandwidth of the high NA objective, allowing the detection of the maximum possible higher-spatial information on the fluorescent object without introducing many artifacts caused by a frequency domain mismatch. Depending on the detection bandwidth of the imaging system and the desired *k*-space, the size of the nanodiscs (or nanoparticles) could be 20−80 nm with a pitch size of 50−200 nm. The fabrication process for the fused silica LPSIM substrate with 60 nm silver nanoantennas and a 150 nm pitch size was published previously.[29]

Fabrication Process for Sapphire LPSIM Substrates. The fabrication starts with a 1 in. sapphire coverslip from Olympus as a substrate. Electron-beam lithography is used to define the pillar array pattern on the substrate with PMMA as a resist. In order to avoid charging effects disturbing the exposure, a thin layer of ITO is deposited on the substrate before coating with PMMA. After the exposure and development of the PMMA, a 60 nm Ag layer is deposited on the substrate following a 2 nm Ge adhesion layer by electron-beam evaporation. The sample is then lifted off in an acetone bath and rinsed in isopropyl alcohol, leaving the pillar array on the substrate. Finally, PMMA is spin-coated on the sample multiple times to planarize the surface. Following each coating, the sample is baked on a 180 °C hot plate for 5 min to remove solvent and reflow the polymer. Figure S1 summarizes the main steps of the fabrication process. We note that a similar process of fabrication can be used with other types of coverslips, different periodic patterns, and metals.

The fabricated sapphire LPSIM substrate has multiple 1 mm^2 hexagonal lattice patterns of silver discs (60 nm in diameter and height) with 125, 135, and 145 nm pitch sizes (Figure 3a−c) embedded in PMMA. The pitch and nanodisc size can be defined by the electron-beam lithography step. The thin top layer of PMMA protects the silver nanodiscs and creates a relatively flat surface for biological surface imaging while keeping the sample in the range of the evanescent plasmonic field. To minimize near-field coupling between evanescent waves from neighboring nanodiscs, the ratio between disc height, diameter, and pitch size was estimated by simulating near-field excitation patterns on objects at different incidental illumination angles (Figure 3d).

After experimental usage or damage of the substrate, the PMMA protection layer with any attached loose fluorescence can be removed by using acetone, and new PMMA protection layers can be spin-coated. By recoating new protection layers, the same substrate can be used multiple times without contamination of the sample or damaging the substrate.

Microtubulin Preparation for Fluorescence Microscopy. The chemicals for microtubules were purchased from Cytoskeleton, Inc. The modified preparation protocol is provided as Supporting Information. Prepared microtubules were diluted to proper concentration, drop-casted onto the LPSIM substrate, and sandwiched with a regular coverslip glass.

Image Processing. All of our video frame processing and reconstructions were performed with MATLAB software. Before LPSIM reconstruction, image sectioning for subimages was performed so that out-of-plane noise due to fluorophores excited by direct transmitted laser light rather than plasmonic field will be suppressed in the reconstructed image. Because the illumination pattern of LPSIM is not a sinusoidal standing wave in traditional SIM and the actual illumination pattern in experiment might have distortions caused by fabrication uncertainties, we used the blind SIM[35] reconstruction approach, which does not require exact knowledge of the illumination pattern. Instead of calculating the object information in Fourier space, both the object and the illumination patterns are treated as unknowns in real space and are solved using a cost-minimization strategy. Each super-resolution LPSIM frame is reconstructed using nine subimages with different illumination angles.

ASSOCIATED CONTENT

Supporting Information

The Supporting Information is available free of charge on the ACS Publications website at DOI: 10.1021/acsnano.8b03477.

Additional details on experimental methods; figures showing fabrication steps for sapphire LPSIM substrates and a graph of ideal fwhm of beads on top of the LPSIM substrate; protocol of microtubulin preparation for fluorescent microscopy (PDF)

Movie S1 showing super-resolution and diffraction-limited 4 Hz video recordings of green microtubule dynamics on a silica-based LPSIM substrate (AVI)

Movie S2 showing the process of how a microtubule breaks apart in time (AVI)

Movie S3 showing a short 1 Hz super-resolution video of microtubule dynamics on a sapphire-based LPSIM substrate (AVI)

AUTHOR INFORMATION

Corresponding Author

*E-mail: zhaowei@ucsd.edu.

ORCID

Anna Bezryadina: 0000-0002-9776-5477

Author Contributions

Z.L., A.B., and J.Z. conceived the project and wrote the manuscript. A.B. and J.Z. performed the experiments, prepared samples, and analyzed data. A.B. modified the optical system. J.Z. wrote software and prepared silica substrates. Y.X. prepared sapphire substrates. All authors advised and edited the manuscript. Z.L. supervised the research.

Notes

The authors declare no competing financial interest.

ACKNOWLEDGMENTS

We thank E. Huang, Q. Ma, and J. Ponsetto for assistance with LPSIM substrate fabrication and for comments, and Hu Cang for assistance with microtubule sample preparation. The work was supported by the Gordon and Betty Moore Foundation and the National Science Foundation CBET-1604216.

REFERENCES

(1) Schermelleh, L.; Heintzmann, R.; Leonhardt, H. A Guide to Super-Resolution Fluorescence Microscopy. *J. Cell Biol.* **2010**, *190*, 165−175.

(2) Lukinavičius, G.; Umezawa, K.; Olivier, N.; Honigmann, A.; Yang, G.; Plass, T.; Mueller, V.; Reymond, L.; Corrêa, I. R., Jr.; Luo, Z. G.; et al. A Near-Infrared Fluorophore for Live-Cell Super-Resolution Microscopy of Cellular Proteins. *Nat. Chem.* **2013**, *5*, 132−139.

(3) Hein, B.; Willig, K. I.; Hell, S. W. Stimulated Emission Depletion (STED) Nanoscopy of a Fluorescent Protein-Labeled Organelle inside a Living Cell. *Proc. Natl. Acad. Sci. U. S. A.* **2008**, *105*, 14271−14276.

(4) Lukinavičius, G.; Reymond, L.; D'este, E.; Masharina, A.; Göttfert, F.; Ta, H.; Güther, A.; Fournier, M.; Rizzo, S.; Waldmann, H.; et al. Fluorogenic Probes for Live-Cell Imaging of the Cytoskeleton. *Nat. Methods* **2014**, *11*, 731−733.

(5) Hell, S. W.; Sahl, S. J.; Bates, M.; Zhuang, X.; Heintzmann, R.; Booth, M. J.; Bewersdorf, J.; Shtengel, G.; Hess, H.; Tinnefeld, P.; et al. The 2015 Super-Resolution Microscopy Roadmap. *J. Phys. D: Appl. Phys.* **2015**, *48*, 443001.

(6) Gustafsson, M. G. L. Surpassing the Lateral Resolution Limit by a Factor of Two Using Structured Illumination Microscopy. *J. Microsc.* **2000**, *198*, 82−87.

(7) Kner, P.; Chhun, B. B.; Griffis, E. R.; Winoto, L.; Gustafsson, M. G. L. Super-Resolution Video Microscopy of Live Cells by Structured Illumination. *Nat. Methods* **2009**, *6*, 339−342.

DOI: 10.1021/acsnano.8b03477
ACS Nano XXXX, XXX, XXX−XXX

(8) Willig, K. I.; Harke, B.; Medda, R.; Hell, S. W. STED Microscopy with Continuous Wave Beams. *Nat. Methods* **2007**, *4*, 915−918.
(9) Hell, S. W.; Wichmann, J. Breaking the Diffraction Resolution Limit by Stimulated-Emission: Stimulated-Emission-Depletion Fluorescence Microscopy. *Opt. Lett.* **1994**, *19*, 780−782.
(10) Huang, B.; Wang, W. Q.; Bates, M.; Zhuang, X. W. Three-Dimensional Super-Resolution Imaging by Stochastic Optical Reconstruction Microscopy. *Science* **2008**, *319*, 810−813.
(11) Rust, M. J.; Bates, M.; Zhuang, X. W. Sub-Diffraction-Limit Imaging by Stochastic Optical Reconstruction Microscopy (STORM). *Nat. Methods* **2006**, *3*, 793−795.
(12) Betzig, E.; Patterson, G. H.; Sougrat, R.; Lindwasser, O. W.; Olenych, S.; Bonifacino, J. S.; Davidson, M. W.; Lippincott-Schwartz, J.; Hess, H. F. Imaging Intracellular Fluorescent Proteins at Nanometer Resolution. *Science* **2006**, *313*, 1642−1645.
(13) Schermelleh, L.; Carlton, P. M.; Haase, S.; Shao, L.; Winoto, L.; Kner, P.; Burke, B.; Cardoso, M. C.; Agard, D. A.; Gustafsson, M. G.; et al. Subdiffraction Multicolor Imaging of the Nuclear Periphery with 3D Structured Illumination Microscopy. *Science* **2008**, *320*, 1332−1336.
(14) Blau, Y.; Shterman, D.; Bartal, G.; Gjonaj, B. Double Moiré Structured Illumination Microscopy with High-Index Materials. *Opt. Lett.* **2016**, *41*, 3455−3458.
(15) Li, D.; Shao, L.; Chen, B. C.; Zhang, X.; Zhang, M.; Moses, B.; Milkie, D. E.; Beach, J. R.; Hammer, J. A.; Pasham, M.; et al. Extended-Resolution Structured Illumination Imaging of Endocytic and Cytoskeletal Dynamics. *Science* **2015**, *349*, aab3500.
(16) Keller, P. J.; Schmidt, A. D.; Santella, A.; Khairy, K.; Bao, Z.; Wittbrodt, J.; Stelzer, E. H. Fast, High-Contrast Iimaging of Animal Development with Scanned Light Sheet-Based Structured-Illumination Microscopy. *Nat. Methods* **2010**, *7*, 637−642.
(17) York, A. G.; Chandris, P.; Dalle Nogare, D.; Head, J.; Wawrzusin, P.; Fischer, R. S.; Chitnis, A.; Shroff, H. Instant Super-Resolution Imaging in Live Cells and embryos *via* Analog Image Processing. *Nat. Methods* **2013**, *10*, 1122−1126.
(18) Gustafsson, M. G. L. Nonlinear Structured-Illumination Microscopy: Wide-Field Fluorescence Imaging with Theoretically Unlimited Resolution. *Proc. Natl. Acad. Sci. U. S. A.* **2005**, *102*, 13081−13086.
(19) Rego, E. H.; Shao, L.; Macklin, J. J.; Winoto, L.; Johansson, G. A.; Kamps-Hughes, N.; Davidson, M. W.; Gustafsson, M. G. Nonlinear Structured-Illumination Microscopy with a Photoswitchable Protein Reveals Cellular Structures at 50-nm Resolution. *Proc. Natl. Acad. Sci. U. S. A.* **2012**, *109*, E135−E143.
(20) Heintzmann, R.; Jovin, T. M.; Cremer, C. Saturated Patterned Excitation Microscopy - a Concept for Optical Resolution Improvement. *J. Opt. Soc. Am. A* **2002**, *19*, 1599−1609.
(21) Heintzmann, R.; Gustafsson, M. G. L. Subdiffraction Resolution in Continuous Samples. *Nat. Photonics* **2009**, *3*, 362−364.
(22) Willets, K. A.; Wilson, A. J.; Sundaresan, V.; Joshi, P. B. Super-Resolution Imaging and Plasmonics. *Chem. Rev.* **2017**, *117*, 7538−7582.
(23) Ströhl, F.; Kaminski, C. F. Frontiers in Structured Illumination Microscopy. *Optica* **2016**, *3*, 667−677.
(24) Wei, F.; Lu, D.; Shen, H.; Wan, W.; Ponsetto, J. L.; Huang, E.; Liu, Z. Wide Field Super-Resolution Surface Imaging through Plasmonic Structured Illumination Microscopy. *Nano Lett.* **2014**, *14*, 4634−4639.
(25) Wei, F.; Liu, Z. Plasmonic Structured Illumination Microscopy. *Nano Lett.* **2010**, *10*, 2531−2536.
(26) Wang, Q.; Bu, J.; Tan, P. S.; Yuan, G. H.; Teng, J. H.; Wang, H.; Yuan, X. C. Subwavelength-Sized Plasmonic Structures for Wide-Field Optical Microscopic Imaging with Super-Resolution. *Plasmonics* **2012**, *7*, 427−433.
(27) Fernández-Domínguez, A. I.; Liu, Z.; Pendry, J. B. Coherent Four-Fold Super-Resolution Imaging with Composite Photonic−Plasmonic Structured Illumination. *ACS Photonics* **2015**, *2*, 341−348.
(28) Ponsetto, J. L.; Wei, F.; Liu, Z. Localized Plasmon Assisted Structured Illumination Microscopy for Wide-Field High-Speed Dispersion-Independent Super Resolution Imaging. *Nanoscale* **2014**, *6*, 5807−5812.
(29) Ponsetto, J. L.; Bezryadina, A.; Wei, F.; Onishi, K.; Shen, H.; Huang, E.; Ferrari, L.; Ma, Q.; Zou, Y.; Liu, Z. Experimental Demonstration of Localized Plasmonic Structured Illumination Microscopy. *ACS Nano* **2017**, *11*, 5344−5350.
(30) Bezryadina, A.; Li, J.; Zhao, J.; Kothambawala, A.; Ponsetto, J.; Huang, E.; Wang, J.; Liu, Z. Localized Plasmonic Structured Illumination Microscopy with an Optically Trapped Microlens. *Nanoscale* **2017**, *9*, 14907−14912.
(31) Purcell, E. M. Spontaneous Emission Probabilities at Radio Frequencies. *Phys. Rev.* **1946**, *69*, 681.
(32) Cang, H.; Liu, Y.; Wang, Y.; Yin, X.; Zhang, X. Giant Suppression of Photobleaching for Single Molecule Detection *via* the Purcell Effect. *Nano Lett.* **2013**, *13*, 5949−5953.
(33) Tam, F.; Goodrich, G. P.; Johnson, B. R.; Halas, N. J. Plasmonic Enhancement of Molecular Fluorescence. *Nano Lett.* **2007**, *7*, 496−501.
(34) Neil, M. A. A.; Juškaitis, R.; Wilson, T. Method of Obtaining Optical Sectioning by Using Structured Light in a Conventional Microscope. *Opt. Lett.* **1997**, *22*, 1905−1907.
(35) Mudry, E.; Belkebir, K.; Girard, J.; Savatier, J.; Le Moal, E.; Nicoletti, C.; Allain, M.; Sentenac, A. Structured Illumination Microscopy Using Unknown Speckle Patterns. *Nat. Photonics* **2012**, *6*, 312−315.

DOI: 10.1021/acsnano.8b03477
ACS Nano XXXX, XXX, XXX−XXX